J|A|C|S

Communication

High Performance Reduction of H_2O_2 with an Electron Transport Decaheme Cytochrome on a Porous ITO Electrode

Bertrand Reuillard,[†] Khoa H. Ly,[†] Peter Hildebrandt,[‡] Lars J. C. Jeuken,*,[§] Julea N. Butt,*,[#] and Erwin Reisner*,[†]

[†]Department of Chemistry, University of Cambridge, Lensfield Road, Cambridge CB2 1EW, United Kingdom
[‡]Institut für Chemie, Technische Universität Berlin, Sekr. PC14, Straße des 17. Juni 135, D-10623 Berlin, Germany
[§]School of Biomedical Sciences and the Astbury Centre, University of Leeds, Leeds LS2 9JT, United Kingdom
[#]School of Chemistry and School of Biological Sciences, University of East Anglia, Norwich Research Park, Norwich NR4 7TJ, United Kingdom

S *Supporting Information*

ABSTRACT: The decaheme cytochrome MtrC from *Shewanella oneidensis* MR-1 immobilized on an ITO electrode displays unprecedented H_2O_2 reduction activity. Although MtrC showed lower peroxidase activity in solution compared to horseradish peroxidase, the ten heme cofactors enable excellent electronic communication and a superior activity on the electrode surface. A hierarchical ITO electrode enabled optimal immobilization of MtrC and a high current density of 1 mA cm^{-2} at 0.4 V vs SHE could be obtained at pH 6.5 (E_{onset} = 0.72 V). UV−visible and Resonance Raman spectroelectrochemical studies suggest the formation of a high valent iron-oxo species as the catalytic intermediate. Our findings demonstrate the potential of multiheme cytochromes to catalyze technologically relevant reactions and establish MtrC as a new benchmark in biotechnological H_2O_2 reduction with scope for applications in fuel cells and biosensors.

Electrocatalytic conversion of H_2O_2 has been extensively studied toward the development of (bio)sensors.[1] H_2O_2 has also been suggested as a route to chemical energy storage, offering an alternative to the commonly envisioned hydrogen and methanol.[2,3] The sustainable production of H_2O_2 from water and O_2 using electrocatalytic[4] or photo(electro)-catalytic[5,6] processes is therefore investigated as a viable alternative to water splitting. Several studies have proposed the direct electrocatalytic disproportionation of H_2O_2 on the cathode and anode in a fuel cell.[7,8] Fukuzumi and co-workers studied the use of different types of iron catalysts for the fabrication of cathodes in H_2O_2 fuel cells in water.[9,10]

Biofuel cells that electrically wire redox enzymes on electrodes are also under development, but without adapted orientation or redox mediation strategies low current densities are often obtained due to poor interfacial interactions.[11] Horseradish peroxidase (HRP) is the state-of-the-art biocatalyst for H_2O_2 electroreduction and has been widely employed in H_2O_2 sensing[12] as well as for H_2O_2 reduction in O_2 reducing biocathodes.[13,14] A high potential Fe^{IV}=O state of the protoporphyrin IX (hemin) cofactor in HRP has been

suggested to be responsible for its activity.[15] The presence of histidine and arginine in the outer coordination sphere of the iron center stabilizes the high potential intermediate at around 0.9 V vs SHE.[16]

MtrC is a decaheme protein and part of the protein complex MtrCAB that can be found in the outer membrane of *Shewanella oneidensis* MR-1.[17] Within the organism, MtrCAB is known to act as an electron conduit from the intracellular to the extracellular environment, where MtrC can transfer electrons to different acceptors, such as metal oxides and flavins.[18] A crystal structure of MtrC shows all ten hemes with axial ligation by two histidine residues (Figures 1 and S1).[19]
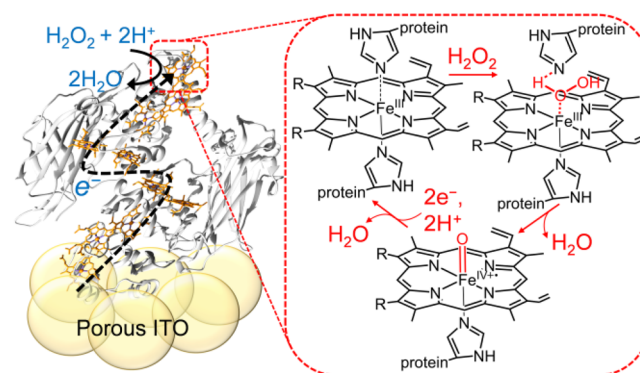

Figure 1. Schematic representation of the electronic communication between MtrC and a porous ITO electrode with the proposed mechanism for the peroxidase activity based on the HRP catalytic cycle. The catalytic site in MtrC has been arbitrarily assigned.

We investigated the potential peroxidase activity of MtrC when immobilized onto porous ITO electrodes (Figure 1) by protein film electrochemistry and spectroelectrochemistry (SEC). MtrC was immobilized by dropcasting 5 μL of a 40 μM solution onto a mesostructured ITO (mesoITO) electrode (0.25 cm², ~3 μm thick, ~50 nm size of ITO particles, see SI). Protein film voltammetry (PFV) scans of mesoITO|MtrC recorded at different scan rates show a broad and reversible
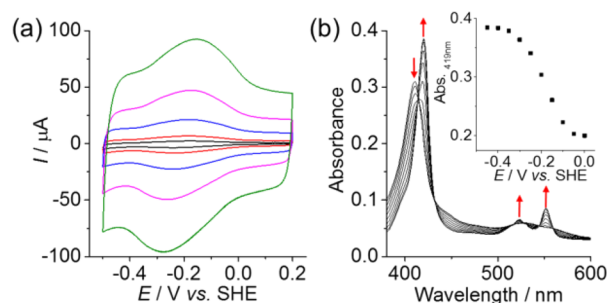
Figure 2. (a) PFV scans of MtrC immobilized on a mesoITO electrode at different scan rates (10, 20, 50, 100, and 200 mV s^{-1}). (b) UV–vis SEC of a mesoITO|MtrC electrode following the reduction of Fe^{III} to Fe^{II}-heme (at 0, −0.05, −0.10, −0.15, −0.20, −0.25, −0.30, −0.35, −0.4, and −0.45 V vs SHE). (Inset) Absorbance at 419 nm as a function of E_{app}. All experiments were performed in MES solution (0.1 M) at pH 6.5 and 20 °C.

redox wave at $E_{1/2}$ = −0.21 V (all redox potentials quoted vs SHE), characteristic of the ten successive Fe^{III}/Fe^{II} redox couples of the hemes within MtrC (Figure 2a).[20] The peak currents show a linear dependence with scan rate confirming the immobilization of the protein (Figure S2). Integration of the Fe^{II}→Fe^{III} oxidation wave allowed calculation of the charge per geometrical surface area yielding 1.9 nmol heme per cm^2, corresponding to 0.19 nmol MtrC per cm^2.

UV–vis SEC measurements were carried out and showed that MtrC remains in the fully oxidized state on mesoITO at positive potentials with a sharp band at 410 nm and a broader feature around 500 to 600 nm (Figure 2b). At more negative potentials new signals at 419, 524, and 552 nm appeared, corresponding to the formation of the reduced Fe^{II}-hemes in MtrC.[20] The disappearance of Fe^{III}-heme bands at E < −0.35 V indicates that the majority of heme cofactors in the adsorbed MtrC are in electronic communication with the ITO via direct electron transfer (DET) or a combination of inter- and intramolecular electron transfer events.

Addition of H$_2$O$_2$ (5 mM) to the electrolyte solution caused a substantial increase of the open circuit potential (OCP) for the mesoITO|MtrC electrode from 0.37 to 0.75 V (Figure 3a), which is close to that reported for Fe^{IV}=O of peroxidase active sites and suggests the formation of a high oxidation state intermediate.[16] The free cofactor, hemin, and HRP were also immobilized on mesoITO electrodes. Upon addition of H$_2$O$_2$, the OCP increased from 0.45 to 0.61 V for mesoITO|hemin (7.5 nmol hemin per cm^2; Figure S3), and mesoITO|HRP showed only a modest increase from 0.42 to 0.46 V, probably due to unfavorable enzyme orientation (Figure 3a).

The potential peroxidase activity of MtrC was studied using PFV in the presence of H$_2$O$_2$ (Figure 3b). An intense catalytic wave was observed with mesoITO|MtrC with an electro-catalytic onset potential (E_{onset}) of 0.72 V for the reduction of H$_2$O$_2$, comparable to values observed for the reduction of H$_2$O$_2$ by HRP on carbon electrode surfaces.[13,14] A strong catalytic oxidation wave at the same E_{onset} was observed, which can be attributed to the oxidation of H$_2$O$_2$. Control experiments with mesoITO in the absence of MtrC revealed only a minor wave at E_{onset} = 0.35 V (Figure S4).

The mesoITO|hemin electrode displayed significantly smaller current densities with H$_2$O$_2$ at a less positive E_{onset} of 0.61 V (Figure 3b), despite a 4× higher cofactor loading compared to mesoITO|MtrC. As expected from the OCP measurements, the
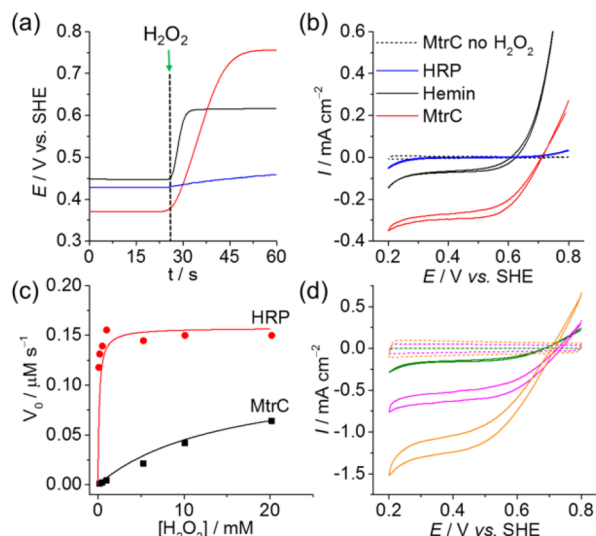
Figure 3. (a) OCP measurements of MtrC (red trace), hemin (black trace), and HRP (blue trace) immobilized onto a mesoITO electrode upon addition of H$_2$O$_2$ (5 mM). (b) Voltammograms recorded in the absence (dashed trace) and presence of H$_2$O$_2$ (5 mM) with MtrC, free hemin, and HRP immobilized onto mesoITO (ν = 20 mV s^{-1}). (c) Initial velocity (V_o) of ABTS$^{+\bullet}$ formation measured by UV–visible spectrophotometry for solutions of MtrC (10 nM) or HRP (10 nM) following the addition of H$_2$O$_2$ (0.1, 0.2, 0.5, 1, 5, 10, and 20 mM) in the presence of ABTS (2 mM). (d) PFV scans with MtrC immobilized onto IOmesoITO electrodes of 2 μm thick (green trace), 12 μm (purple trace), and 20 μm (orange trace) (ν = 20 mV s^{-1}). All experiments were performed in aqueous MES solution (0.1 M) at pH 6.5 and 20 °C.

HRP modified mesoITO electrode showed almost no electro-catalytic activity with H$_2$O$_2$. Nevertheless, addition of 2,2′-azino-bis(3-ethylbenzothiazoline-6-sulfonic acid), ABTS (1 mM), as a redox mediator between HRP and electrode led to catalytic currents from H$_2$O$_2$ reduction (Figure S5a). This indicates that HRP has been immobilized on ITO, but DET is impeded by an unfavorable enzyme orientation.

Chronoamperometry (CA) was carried out with mesoITO|MtrC at an applied electrochemical potential (E_{app}) of 0.4 V (Figure S6) with different amounts of H$_2$O$_2$. From these measurements, K_M^{app} was determined to be ∼1.5 mM, higher than the K_M reported for HRP.[14] The current density reached a maximum value of −200 ± 5 μA cm^{-2} with H$_2$O$_2$ (11 mM), which gives access to an electrochemical k_{cat} of 5 s^{-1} (see SI for calculation). Addition of ABTS (1 mM) does not increase the catalytic activity of H$_2$O$_2$ reduction, indicating that MtrC is already efficiently wired to mesoITO electrode (Figure S5b).

The ability of MtrC to oxidize ABTS in solution was also studied and compared to HRP. ABTS is oxidized by Fe^{IV}=O, yielding a deep green color with a characteristic absorption band at 415 nm and shoulders around 650 and 750 nm.[14] When H$_2$O$_2$ (20 mM) was added to a solution of MtrC (80 nM) and ABTS (10 mM), an intense signal appeared at the expected wavelength (Figure S7a). This experiment supports the formation of a high potential Fe^{IV}=O within the MtrC structure that resembles the active species in HRP. Kinetic studies in the presence of ABTS (2 mM) and increasing amounts H$_2$O$_2$ recording the appearance of ABTS$^{+\bullet}$ by UV–vis spectrophotometry at 415 nm show that MtrC displays a significantly lower activity than HRP for the oxidation of ABTS at saturating concentrations of H$_2$O$_2$ (Figure 3c). From these

kinetic measurements and equations presented in the SI, a k_{cat} for HRP of 7 s^{-1} was calculated, which is somewhat lower than previously reported for HRP.[21] MtrC displayed a k_{cat} of 3 s^{-1}.

As MtrC reduced H$_2$O$_2$ at a low overpotential, the protein (5 μL of 40 μM solution) was immobilized onto a hierarchical inverse opal (IO) mesoITO electrode (750 nm pore diameter, ~50 nm size particles; see SI for details) with a morphology optimized for protein loading in order to maximize current densities. PFV scans performed with IOmesoITO|MtrC show the expected broad reversible redox signals from the Fe^{III}/Fe^{II} couple in MtrC at $E_{1/2}$ of −0.20 V (Figure S8a). The enzyme loading grows linearly with the IOmesoITO film thickness and the calculated surface concentrations of MtrC are 0.15, 0.59, and 0.82 nmol cm^{-2} on 2, 12, and 20 μm thick IOmesoITO electrodes, respectively (Figure S8b). This increase in protein loading led to higher catalytic currents in the PFV scans, reaching −1.5 mA cm^{-2} for the 20 μm thick IO electrode at E = 0.2 V (Figure 3d). The E_{onset} (0.7 V) is similar to those observed with mesoITO|MtrC. The same trend is observed in the CA measurement at E_{app} = 0.4 V (Figure S8c). Maximum current densities of 0.13, 0.47, and 0.96 mA cm^{-2} are obtained for 2, 12, and 20 μm thick electrodes respectively, highlighting the excellent wiring of MtrC on IOmesoITO electrodes to perform peroxidase activity. For 20 μm thick IOmesoITO| MtrC, 30% of the initial catalytic current remained after 1 h of CA at 0.4 V (Figure S8d).

Confocal RR spectroscopy was used to obtain structural insights into the protein integrity and heme environment of MtrC in solution and adsorbed onto ITO as well as in the presence of H$_2$O$_2$. Excitation at 413 nm afforded intense RR spectra in the region from 1300 to 1700 cm^{-1}, dominated by the heme marker modes ν_4, ν_3, ν_2, and ν_{10}, indicating the heme's oxidation, coordination, and spin state.[22] Potentiometric RR titration from +0.2 to −0.55 V shows that the vast majority of the heme groups are redox active and reduced upon applying a cathodic potential, demonstrated by the appearance of marker bands of the reduced heme species (Figure 4). Comparison of MtrC RR spectra in solution and on ITO shows no significant spectral differences (Figure S9b), which supports that the heme environment is not distorted upon adsorption of MtrC onto ITO (Figure 4b).
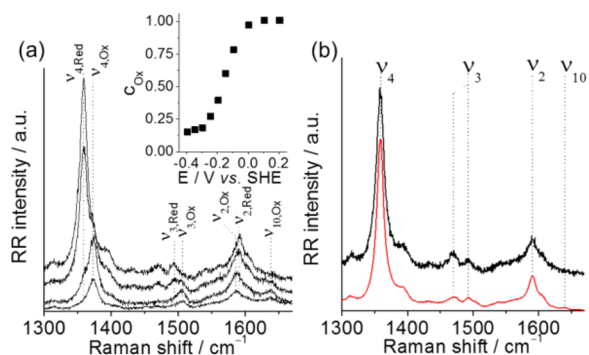
Figure 4. (a) RR SEC of mesoITO|MtrC at different E_{app} (0.2, 0, −0.15, and −0.25 V vs SHE). The inset shows the calculated relative concentration of oxidized bis-histidine ligated hemes c_{ox} as a function of potential. (b) Comparison of the RR spectra of ferrous MtrC under 413 nm excitation in solution (red trace) and on mesoITO (black trace). All experiments were performed in MES solution (0.1 M) at pH 6.5 and room temperature in the absence of H$_2$O$_2$.

Component fit analysis was employed to deconvolute the spectral contributions of different heme species (Figure S9, details of the fitting process are given in the SI).[23,24] The dominating species with marker bands located at 1375, 1506, and 1639 cm^{-1} in the ferric and 1359, 1491, and 1621 cm^{-1} in the ferrous state for ν_4, ν_3, and ν_{10}, respectively, is assigned to hexacoordinated hemes with bis-histidine axial ligation as anticipated from the crystal structure (Table S1).[19,23,25] For these spectral features, the relative concentration of ferric (c_{ox}) with respect to the ferrous form was calculated and plotted versus the applied potential (Figure 4a, inset). The midpoint potential of the spectral change was −0.16 V; close to the −0.19 V obtained by electronic absorbance and −0.21 V by PFV (Figure 2).

In addition to the main hexacoordinated low spin species, the spectral analysis revealed the presence of a heme species exhibiting downshifted marker bands at 1371, 1502, and 1636 cm^{-1} for ν_4, ν_3, and ν_{10} in the ferric state, respectively (Table S1). The low-frequency shift indicates a different heme ligation state that cannot be explained by a mere change of the axial ligands. A more plausible explanation is that this species is characterized by a more loosely bound sixth (histidine) axial ligand causing either a distortion of the heme plane or an intermediate spin state in the heme. Both scenarios would result in a frequency downshift when compared to the RR signature from conventional His/His ligated hemes (see SI).[25−27] Importantly, this observation is indicative of a weakened bond between one axial ligand and iron. Such a situation may facilitate coordination of H$_2$O$_2$ by displacement of the loosely bound histidine to enable the peroxidase catalytic activity of MtrC (Scheme S1). Similar observations have been made for other proteins with hexacoordinated heme groups.[28,29] In this respect, the displaced histidine group in the outer coordination sphere of the active site of MtrC may promote proton transfer or stabilize the bound substrate as previously reported for HRP.[15] A weak coordination of one histidine in a fraction of the cofactors is in line with the concomitant observation of a reversibly formed ferrous pentacoordinated heme upon reduction for both MtrC adsorbed and in solution (Figure 4b), evidenced by the ν_3 mode at 1471 cm^{-1} (see SI).[26,27] Its 4- to 5-fold lower contribution to the RR spectrum than noted for the bis-histidine species further implies that one or two of the ten heme groups in MtrC exhibit the altered binding situation allowing access for H$_2$O$_2$.

RR spectra recorded under turnover conditions monitored the influence of H$_2$O$_2$ (5 mM) on the heme environment. The spectra recorded at E_{app} of 0.2 and 0.7 V were identical to those recorded under nonturnover conditions, indicating that the heme environment is not effectively altered upon substrate addition (Figure S10). The absence of a spectral indication for an iron-oxo intermediate, sometimes apparent by an iron−oxygen stretching mode at around 790 cm^{-1}, does not contradict with our interpretation because the iron−oxygen band is very weak, and the ferryl-oxo state exhibits very similar marker bands to the bis-histidine coordinated heme. This species is also expected to be very short-lived in the catalytic cycle and thus cannot significantly contribute to the RR spectrum.[30]

In summary, we have demonstrated the efficient electrical wiring of MtrC onto mesoITO electrodes using PFV, CA, and SEC (UV−vis and RR). MesoITO|MtrC electrodes exhibit an unforeseen activity toward the reduction of H$_2$O$_2$ at a low

overpotential, which is comparable to the benchmark biocatalyst HRP. SEC of the immobilized MtrC suggests the presence of at least one catalytically active species per protein, assigned to an Fe heme unit with a loosely bound histidine ligand that could form a high-valent iron-oxo species as the catalytic intermediate. Immobilization of MtrC on a large surface area electrode (IOmesoITO) allows for 1 mA cm^{-2} to be achieved at 0.4 V vs SHE, which outperforms HRP and demonstrates the untapped potential of multiheme proteins in the development of H_2O_2 biofuel cells and biosensors.

■ ASSOCIATED CONTENT

Ⓢ Supporting Information

The Supporting Information is available free of charge on the ACS Publications website at DOI: 10.1021/jacs.6b12437.

Experimental Section, Supporting Results, Table S1, Scheme S1, and Figures S1−S9 (PDF)

■ AUTHOR INFORMATION

Corresponding Authors

*l.j.c.jeuken@leeds.ac.uk
*j.butt@uea.ac.uk
*reisner@ch.cam.ac.uk

ORCID Ⓘ

Peter Hildebrandt: 0000-0003-1030-5900
Lars J. C. Jeuken: 0000-0001-7810-3964
Erwin Reisner: 0000-0002-7781-1616

Notes

The authors declare no competing financial interest.
Additional data related to this publication are available at the University of Cambridge data repository (https://doi.org/10.17863/CAM.8047).

■ ACKNOWLEDGMENTS

■ REFERENCES

(1) Wang, J. Chem. Rev. **2008**, 108, 814.
(2) Disselkamp, R. S. Energy Fuels **2008**, 22, 2771.
(3) Fukuzumi, S. Biochim. Biophys. Acta, Bioenerg. **2016**, 1857, 604.
(4) Fellinger, T.-P.; Hasché, F.; Strasser, P.; Antonietti, M. J. Am. Chem. Soc. **2012**, 134, 4072.
(5) Kofuji, Y.; Isobe, Y.; Shiraishi, Y.; Sakamoto, H.; Tanaka, S.; Ichikawa, S.; Hirai, T. J. Am. Chem. Soc. **2016**, 138, 10019.
(6) Mase, K.; Yoneda, M.; Yamada, Y.; Fukuzumi, S. ACS Energy Lett. **2016**, 1, 913.
(7) Shaegh, S. A. M.; Nguyen, N.-T.; Ehteshami, S. M. M.; Chan, S. H. Energy Environ. Sci. **2012**, 5, 8225.
(8) Fukuzumi, S.; Yamada, Y. ChemElectroChem **2016**, 3, 1978.
(9) Yamada, Y.; Yoshida, S.; Honda, T.; Fukuzumi, S. Energy Environ. Sci. **2011**, 4, 2822.
(10) Yamada, Y.; Yoneda, M.; Fukuzumi, S. Energy Environ. Sci. **2015**, 8, 1698.
(11) Cooney, M. J.; Svoboda, V.; Lau, C.; Martin, G.; Minteer, S. D. Energy Environ. Sci. **2008**, 1, 320.
(12) Ferapontova, E. E. Electroanalysis **2004**, 16, 1101.
(13) Jia, W.; Jin, C.; Xia, W.; Muhler, M.; Schuhmann, W.; Stoica, L. Chem. - Eur. J. **2012**, 18, 2783.
(14) Reuillard, B.; Le Goff, A.; Holzinger, M.; Cosnier, S. J. Mater. Chem. B **2014**, 2, 2228.
(15) Berglund, G. I.; Carlsson, G. H.; Smith, A. T.; Szöke, H.; Henriksen, A.; Hajdu, J. Nature **2002**, 417, 463.
(16) Battistuzzi, G.; Bellei, M.; Bortolotti, C. A.; Sola, M. Arch. Biochem. Biophys. **2010**, 500, 21.
(17) Breuer, M.; Rosso, K. M.; Blumberger, J.; Butt, J. N. J. R. Soc., Interface **2015**, 12, 20141117.
(18) Shi, L.; Dong, H.; Reguera, G.; Beyenal, H.; Lu, A.; Liu, J.; Yu, H.-Q.; Fredrickson, J. K. Nat. Rev. Microbiol. **2016**, 14, 651.
(19) Edwards, M. J.; White, G. F.; Norman, M.; Tome-Fernandez, A.; Ainsworth, E.; Shi, L.; Fredrickson, J. K.; Zachara, J. M.; Butt, J. N.; Richardson, D. J.; Clarke, T. A. Sci. Rep. **2015**, 5, 11677.
(20) Lee, C.-Y.; Reuillard, B.; Sokol, K. P.; Laftsoglou, T.; Lockwood, C. W. J.; Rowe, S. F.; Hwang, E. T.; Fontecilla-Camps, J. C.; Jeuken, L. J. C.; Butt, J. N.; Reisner, E. Chem. Commun. **2016**, 52, 7390.
(21) Rodríguez-López, J. N.; Gilabert, M. A.; Tudela, J.; Thorneley, R. N. F.; García-Cánovas, F. Biochemistry **2000**, 39, 13201.
(22) Verma, A. L.; Bernstein, H. J. J. Raman Spectrosc. **1974**, 2, 163.
(23) Oellerich, S.; Wackerbarth, H.; Hildebrandt, P. J. Phys. Chem. B **2002**, 106, 6566.
(24) Ly, K. H.; Wisitruangsakul, N.; Sezer, M.; Feng, J.-J.; Kranich, A.; Weidinger, I. M.; Zebger, I.; Murgida, D. H.; Hildebrandt, P. J. Electroanal. Chem. **2011**, 660, 367.
(25) Siebert, F.; Hildebrandt, P. Vibrational Spectroscopy in Life Science; John Wiley & Sons: Hoboken, NJ, 2008.
(26) Weiss, R.; Gold, A.; Terner, J. Chem. Rev. **2006**, 106, 2550.
(27) Smith, K. M. Porphyrins and Metalloporphyrins; Elsevier: Amsterdam, 1975.
(28) Echalier, A.; Brittain, T.; Wright, J.; Boycheva, S.; Mortuza, G. B.; Fülöp, V.; Watmough, N. J. Biochemistry **2008**, 47, 1947.
(29) Frato, K. E.; Walsh, K. A.; Elliott, S. J. Biochemistry **2016**, 55, 125.
(30) Weidinger, I. M. Biochim. Biophys. Acta, Bioenerg. **2015**, 1847, 119.